doi:10.2533/chimia.2015.784 Chimia 69 (2015) 784–788

Seasonal Solar Thermal Absorption Energy Storage Development

Xavier Daguenet-Frick*[a], Paul Gantenbein[a], Mathias Rommel[a], Benjamin Fumey[b], Robert Weber[b], Kanishka Goonesekera[c], and Tommy Williamson[c]

Abstract: This article describes a thermochemical seasonal storage with emphasis on the development of a reaction zone for an absorption/desorption unit. The heat and mass exchanges are modelled and the design of a suitable reaction zone is explained. A tube bundle concept is retained for the heat and mass exchangers and the units are manufactured and commissioned. Furthermore, experimental results of both absorption and desorption processes are presented and the exchanged power is compared to the results of the simulations.

Keywords: Adsorption · Desorption · Falling film tube bundle · Seasonal solar thermal energy storage · Thermochemical heat storage

1. Introduction

Solar thermal energy storage for heating and cooling systems is a priority goal in the renewable energy future.

High thermal losses occurring by the use of sensible thermal energy in materials over the long term, *i.e.* seasonal storage and a low volumetric energy density (typically, water storages) are drawbacks. Therefore, numerous research groups are applying various approaches that aim to reduce the required tank volume assigned for seasonal thermal storage.[1] Phase-change materials (PCM) and thermochemical materials (TCM) are promising approaches with the potential for increased volumetric energy density. In a TCM-based thermal storage system, thermal energy is used to separate the storage medium working pair in its components. Reversing the process releases thermal energy through an exothermal reaction. The storage material composed of two reactants forming a product are usually aqueous salt solutions (NaOH, LiCl, LiBr, *etc.*). A recent overview of sensible, latent and thermochemical storage concepts indicated the specific advantages and disadvantages.[2]

The closed sorption heat storage approach (only heat is exchanged with the environment, no exchange of substances) functions as a continuous but not full cycle liquid state absorption heat pump.[3] The process operates in the planned temperature and pressure range under exclusion of non-condensing gases. No thermal insulation is required for the storage tanks as long as they are kept at room temperature. In fact, except during the loading/unloading operation, no thermal losses occur over the time as it is the case for conventional water storage.

In a first part of this article, the working principle of the thermochemical storage will be described and focus will be put on the heat and mass exchanger, a central component of the facility. The modelling as well as the manufacture and commissioning of the heat and mass exchanger will be presented in a second part. Experimental measurements and results in both absorption and desorption modes will then be shown in a third part.

2. Thermochemical Storage Concept

2.1 *Working Principle*

The absorption/desorption storage concept works with a sorbent (in the present study aqueous sodium hydroxide) and a sorbate (water).[3] In summer, during the charging process, the solar energy provided by the thermal panels is used in the desorber to increase the sorbent concentration (partial evaporation of water from the sodium hydroxide solution under reduced pressure). The water vapour is condensed and releases its latent heat to the environment (through a ground heat exchanger) and the water is stored at room temperature in its liquid phase.

The concentrated sorbent is separately stored at room temperature until winter, when the storage is discharged through operating in the reverse direction. Then, the sorbate is evaporated under reduced pressure in the evaporator using ground heat at a low temperature level. This vapour flows to the absorber and is absorbed by the concentrated sorbent solution, releasing heat at a sufficiently high temperature level to satisfy the building's heating requirements.

Thus, this storage design concept is based upon the thermally driven heat pump principle.

The concept of this storage allows a separation of the power unit (heat and mass exchangers) and the energy unit (reactant and product storage tanks) – like in gas or oil burner thermal energy system sources. Furthermore, because of the seasonally separated process steps of desorption in summer and absorption in winter one heat and mass exchange component for desorption/absorption and one for condensation/evaporation can be used.

As aqueous sodium hydroxide is available at low cost and as water vapour absorption in aqueous sodium hydroxide has a considerably higher volumetric energy density compared to sensible thermal storage systems (theoretically up to six times for a concentration decrease from 50 to 25 %wt), Weber *et al.*[3] investigated a closed sorption heat storage based on sodium hydroxide and water. In the present work, the reaction zone of an absorption/desorption concept with sodium hydroxide (NaOH) and water will be highlighted and investigated, focussing on the design of the core components.

2.2 *Heat and Mass Exchanger Conception*

A compact geometric design of the heat and mass exchangers is essential in order

*Correspondence: Dr. X. Daguenet-Frick[a]
E-mail: Xavier.Daguenet-Frick@spf.ch.
[a]Institute for Solar Technology SPF
University for Applied Sciences-HSR
Oberseestr. 10, CH-8640 Rapperswil, Switzerland
[b]EMPA
Überlandstrasse 129, CH-8600 Dübendorf, Switzerland
[c]Kingspan Environmental Ltd
180 Gilford Road, Portadown,
Craigavon BT63 5LF, UK

to keep the high volumetric energy density benefits of the chosen concept and material. Both the heat and the mass exchanges are directly correlated to the transfer area. For this transfer zone, the falling film technology with horizontal tubes[4] was chosen because of the large contact area between vapour and the liquid fluid as well as the solution mixing that occurs when the droplets fall from one tube to another. That enables the volume of the heat and mass exchanger area to be decreased.[5] In order to facilitate the vapour transfers in the falling film,[6] all non-condensable gases are removed from the reaction zone (tube bundles seated in evacuated container, see Fig. 1).

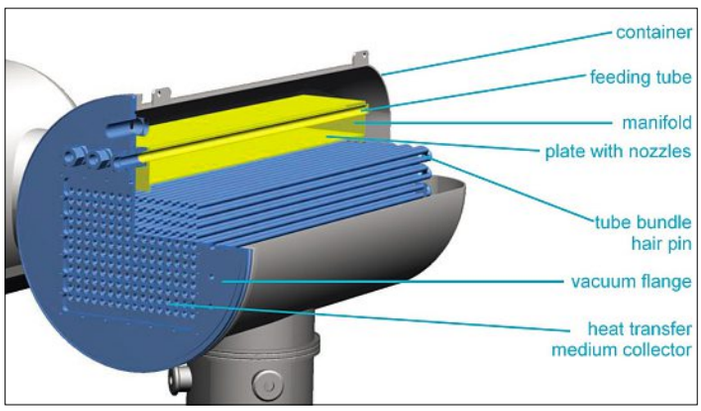

Fig. 1. CAD cross-sectional view of the E/C unit (manifold and tube bundle).

As mentioned above, the sequential running of the heat storage allows a combination of desorption/absorption (A/D) and evaporation/condensation (E/C) processes each confined to one component and an increase of the storage volumetric energy density. However, the challenge in the design of the components is to surmount the different heat and mass transfer rates in the process steps in one component.

A critical point in the design is the homogeneous distribution of the fluids on the outer tube surface to achieve an efficient heat/mass transfer. Therefore, special attention was applied to design the nozzle manifold (in yellow in Fig. 1) that sprays the fluid on the top of the tube bundle. Because of corrosion, stainless steel (DIN 1.4404) is used.

Previous experimental studies on the LiBr-H_2O absorption system showed that a certain degree of fluid recirculation increases the heat and mass transfer. Deng[7] describes that increasing the flow rate (volume flow) per area is favourable for higher heat/mass transfer rates because an improved wetting of the tube surface by a higher volume flow is achieved. Nevertheless, recirculation requires additional electric energy for pumping. To reduce this parasitic energy consumption the challenge is to find a parameter range in which steady state operation can meet the required thermal power without recirculation.

3. Design and Manufacture of the Heat and Mass Exchanger

3.1 *Heat and Mass Exchanger Modelling*

The modelling of the heat and mass exchanger tries to be representative for the reality of the system in regard of the operation set points. In the simulation, the coupled heat, mass and momentum equations are solved under steady state conditions.

The present model considers only one vertical tube column of a falling film heat-exchanger and the scaling of the power is done linearly (fluid distribution inside and outside of the tubes in parallel). For each tube (or horizontal tube row with index n in the scaling, see Fig. 2a), the temperature is calculated inside and outside of the tube, and on the tube surface with the same index as shown in Fig. 2. The heat exchange coefficient (h_i) inside of each tube is calculated according the Sieder and Tate or Colburn correlation depending on the flow regime.[7] For the heat exchange coefficient calculation outside of the tube (h_e), the model convergence was studied using different kinds of correlations. The calculations showed that the prediction of the heat transfer coefficients at low mass flow rates has limited accuracy. For the desorber/absorber sizing, it was therefore

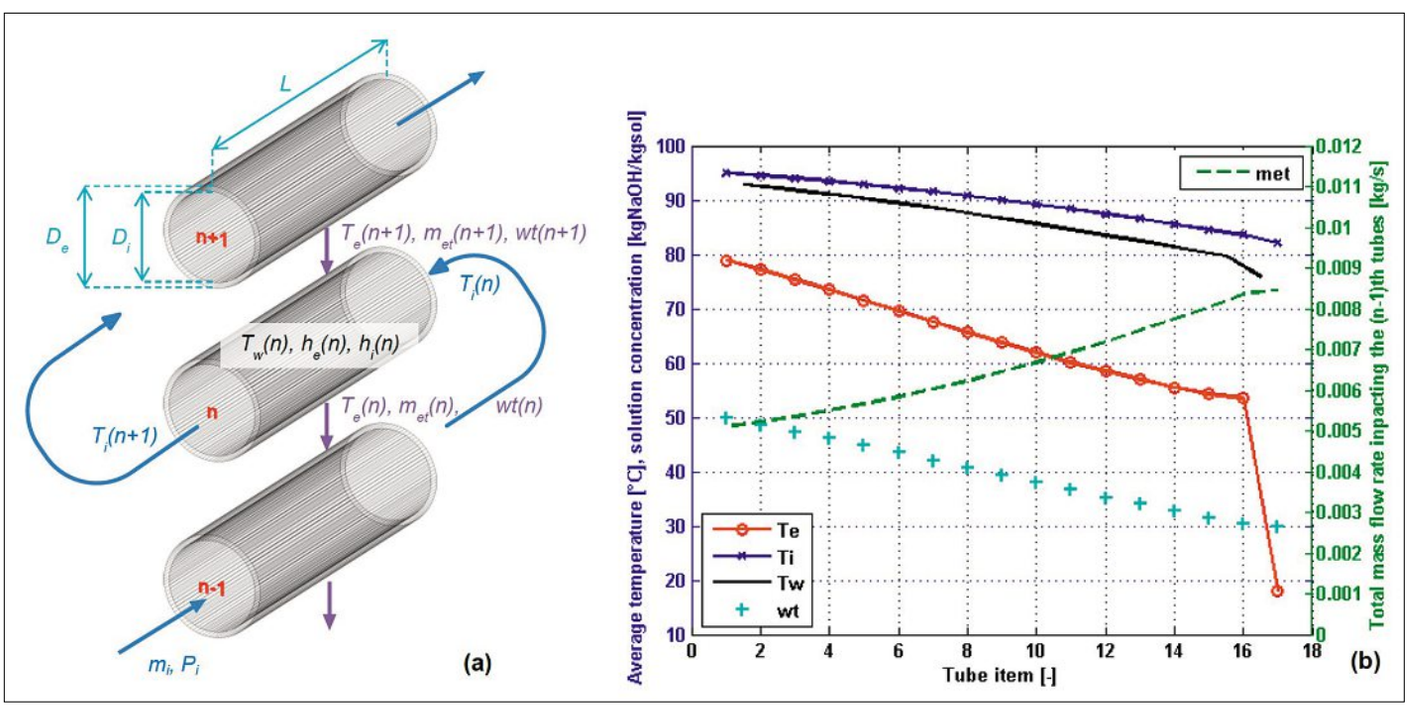

Fig. 2. (a) Tube bundle model schematic with the indicated variables used in the modelling; (b) mass flow rate (right vertical axis), average temperatures and solution concentration (right vertical axis) development in the desorber in function of the tube number n.

decided to use a linear regression based on the experimental data gathered at low mass flow rates by Lee[9] instead of applying the correlations established by Owens[10] and Hu and Jacobi.[11,12]

In the design process a multi-parameter problem has to be solved according to the set boundary conditions. This comprises the definition of the tube bundle geometry: number of tube columns and tube rows, tube length (L), outer and inner tube diameters (D_e, D_i) as well as tube spacing.

Desorber modelling results are shown in Fig. 2b: the development of temperatures (T_e: fluid temperature outside of the tube; T_w: wall temperature; T_i: fluid temperature inside of the tube), of the sodium hydroxide concentration (wt) and of the mass flow rate outside of the tubes (m_{et}) are depicted over a 4×16 tube bundle arrangement in function of tube number n (with bottom-up method enumeration, n=1 is the lowermost tube of the tube bundle). The heat transfer fluid inside the tubes of this counter current heat and mass exchanger, cools down while solar thermal panels heating up this fluid. Outside the tubes, the sorbent is fed by the fluid manifold nozzles with a temperature lower than its saturation temperature. Therefore, T_e raises rapidly until the saturation temperature is reached in uppermost tubes of the tube bundle. Then, partial evaporation occurs, the sorbent concentration (wt) increases and its temperature follows the mixture saturation temperature. As the heat transfer coefficient inside of the tube is higher than outside (see Table 1), the wall temperature T_w is closer to T_i than to T_e.

Table 1 shows that for the desorber/absorber combined heat and mass exchanger unit, the required heat flux (Q) of about 12 kW for the desorber and 8 kW for the absorber is reached with a tube bundle geometry of 4 columns and 18 rows (tube length of L = 300 mm and outside tube diameter of D_e = 10 mm). This tube bundle geometry also minimizes the auxiliary energy consumption of the circulating pump because of moderate pressure losses (calculation inside of the tubes).

In the same way, the tube bundle configuration of the evaporator/condenser unit was determined: 16 columns of 12 rows (same tube diameter D_e, tube length L = 700 mm). In order to increase the heat transfer coefficient outside the tubes, fluid recirculation is planned for the operation of this unit.

Table 1. Modelling of the desorber/absorber unit under the worst working conditions: principle quantities.

		Desorber	Absorber
m_i	[kg/s]	0.300	0.100
T_i(1)	[°C]	95	14
T_i(N+1)	[°C]	80.5	33
h_i	[W/(m²*K)]	7932	2733
P_e	[Pa]	7050	590
m_e(N+1)	[kg/s]	0.0094	0.0048
m_e(1)	[kg/s]	0.0056	0.0080
T_e(N+1)	[°C]	18.0	18.0
T_e(1)	[°C]	79.3	43.0
h_e	[W/(m²*K)]	984	514
Q	[kW]	12.21	7.95

3.2 *Heat and Mass Exchanger Manufacture and Commissioning*

A modular concept (each component is easily dismountable) as well as a limited number of vacuum sealing gaskets were other challenges in the vacuum envelope design. As showed in Fig. 3, two inspection windows allow a view to the top of the tube bundles, which are installed directly under the feed manifold. Except for the both fluid outlets at the bottom of the containers and a temperature sensor feed through in the A/C envelope, all connections and feed throughs are located on the tube bundles flanges (in blue in Fig. 3). These connections enable the feed of the tube manifolds with caustic soda solution on the A/D side and water on the E/C side. Two other feed through connections placed on the flanges are for the evacuation of the containers and the operation pressure measurement. The manifolds are integrated into the flanges for the inlet and outlet of the tube bundles heating and cooling fluid and further feed through are for the temperature sensors measuring the heating and cooling fluid temperature inside the tube bundle tubes as well as outside these tubes (outside tube wall temperatures).

For process and handling reasons as well as for fluid separation, both A/D and E/C units are placed in different containers (Fig. 3). The vapour feed through connects both units, enabling the required exchanges of vapour in both directions (evaporator to absorber or desorber to condenser). On one hand the vapour pressure loss through the feed through should be as low as possible (a value between 50 and 120 Pa is expected depending on the pressure level inside of the reaction zone) and on the other hand the feed through should avoid the transfer of liquid splashes from one container to the other. Additionally, the vapour feed through should only act as mass transfer unit and therefore form a thermal infra-red barrier. A nickel plated and bent metal sheet is implemented for this task and will predominantly form a radiation shield (radiative disconnection due to the high reflectivity of nickel in the infrared).

The manifolds placed at the top of the tube bundle should ensure a homogeneous fluid distribution above the tubes, taking advantage of the experimental results obtained with a preliminary test rig. Particularly tricky was the manufacture of the nozzles in DIN 1.4404 stainless steel alloy. In preference to several other possible designs, a version with nozzles directly machined in a stainless steel nozzles plate was retained. With this version a high flexibility of the nozzle geometry is reached, enabling a good liquid distribution. A drawback of the chosen design is its high price.

Special attention was paid to the fluid distribution on the absorber/desorber tube bundle unit as this heat and mass exchanger is used without fluid recirculation. Like in the preliminary experimentation test rig, the caustic soda mixture enters the

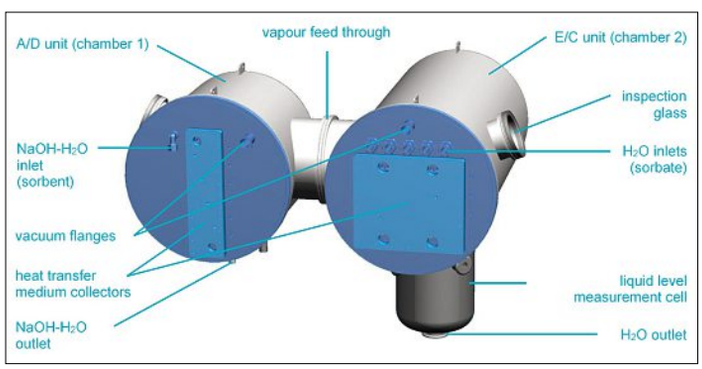

Fig. 3. CAD drawing of the reaction zone with both A/D (left) and E/C unit (right).

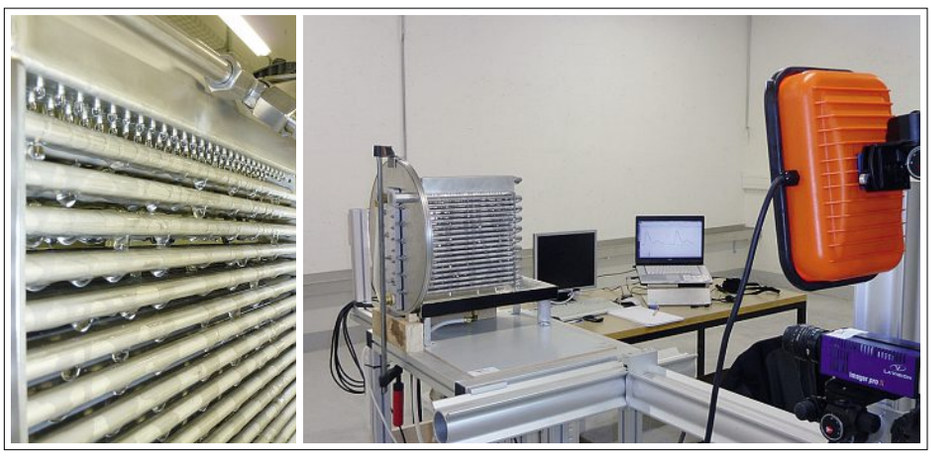

Fig. 4. Side view picture of the falling film on the A/D tube bundle heat and mass exchanger (left) and of the A/D heat and mass heat exchanger during the fluid distribution tests (right).

top of the manifold from both sides of a perforated feed tube. The expected pressure losses through the perforation holes are 3 to 5 time higher than those due to the fluid flow along inside the tube, ensuring an equalised fluid distribution between both ends of the manifold. Furthermore, a fluid film formation is aimed on the bottom plate of the manifold (the plate with the nozzles) ensuring a homogeneous fluid distribution on the manifold nozzles plate on each side of the feed tube. Fig. 4 (left) shows the proper working of the manifold with water as working fluid: the droplets are correctly falling under the nozzles and hit the uppermost tubes of the tube bundle on their total length. An optical method developed to quantify the wetting of the heat and mass exchanger tube arrangement (see Fig. 4, right) also enabled us to validate that the influence of the temperature sensors mounted outside of the tubes (film temperature measurement *Te*) on the fluid flow is small.

4. Measurements

4.1 *Absorption Process*

The first non-isothermal experiment campaign shows that the exchanged power during the discharging process (absorption) is quite a lot lower than expected; only a small concentration decrease of the initial 50wt% sodium hydroxide solution is reached at the outlet of the absorber unit. Therefore, instead of emulating annual operation of a building, it was decided to run measurements in steady state conditions in order to characterize the heat and mass exchangers and to compare the experimental results with those obtained from the numerical modeling. The aim is to find out the weak points of the heat and mass exchangers to further increase the exchanged power value for the absorption process. The measurement points presented in Fig. 5 are averaged values obtained during 30 minutes steady state experiments.

An optical inspection shows that during the discharging process only a fraction (about 50–60%) of the absorber tube bundle surface is wetted. Besides the dependence of the exchanger power on the temperature difference between the evaporator and the absorber (Fig. 5, left), it was also noticed that this power depends on the so-

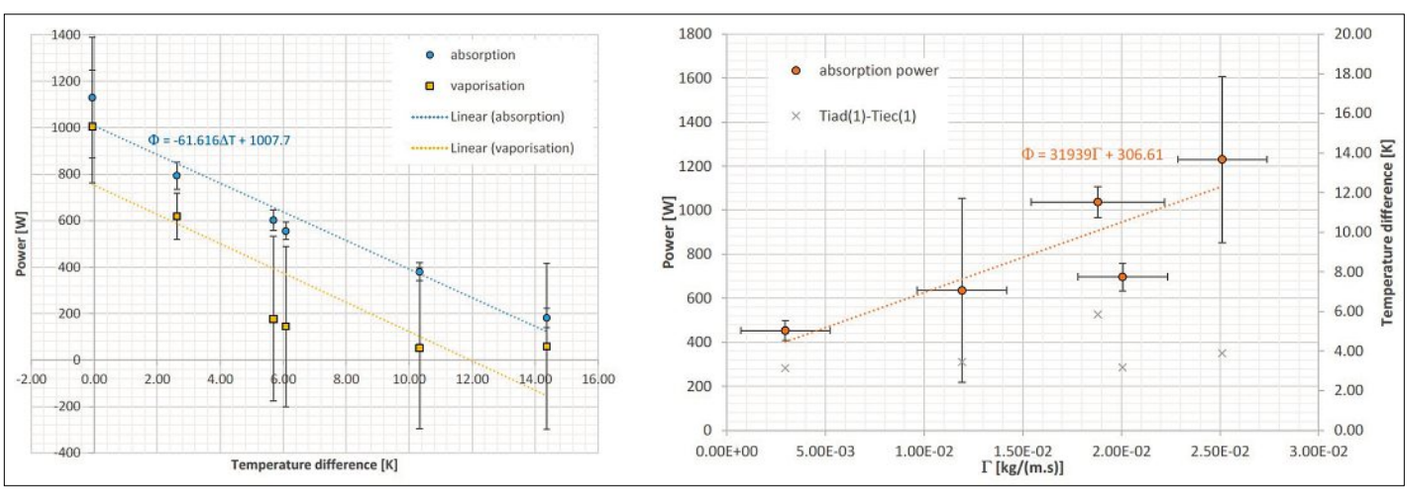

Fig. 5. Development of the power (Φ) in function of the temperature difference (ΔT) between both absorber and evaporator chamber during discharging process (left) and of the absorption power in function of the linear mass flux (Γ) arriving on the absorber (right).

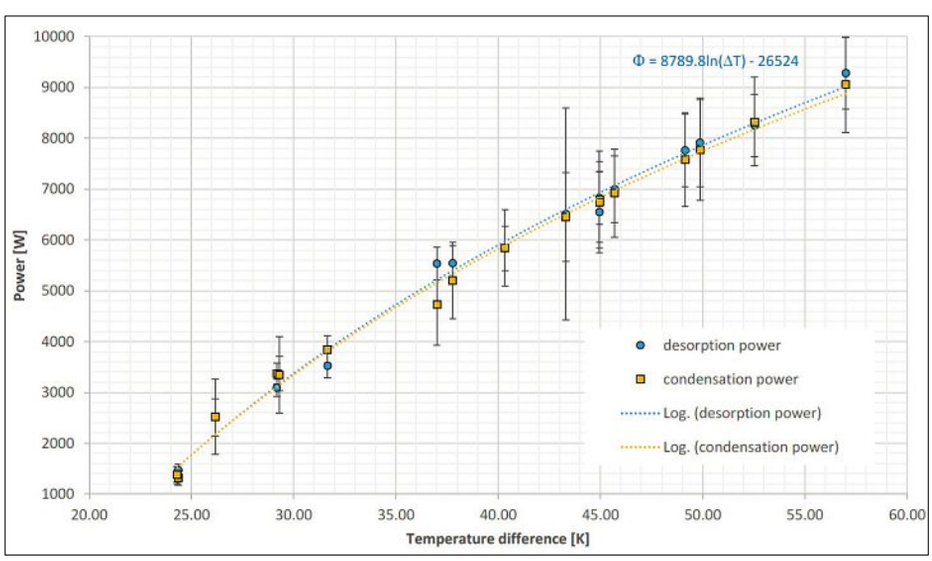

Fig. 6. Development of the power (Φ) in function of the temperature difference (ΔT) between both desorber and condenser chamber during charging process (right).

dium hydroxide mass flux flowing over the absorber (Fig. 5, right). An increase of the sodium lye mass flux leads to a better tube wetting, showing that this parameter is a limiting factor for the exchanged power on the absorber side.

4.2 *Desorption Process*

During the charging process (sorbent desorption with an initial sodium hydroxide concentration of 30wt%), it seems that the exchanged power only depends on the temperature difference between the desorber and the condenser (Fig. 6), a higher temperature difference leads to a higher pressure difference between both units and therefore an increased vapour transfer rate.

The wetting of both tube bundle surfaces as well as the exchanged power on both desorber and condenser are appropriate. For a temperature difference of 60 K (similar to the boundary conditions taken for the modeling), a power of 9.5 kW (about 25 % less than predicted) can be reached.

5. Conclusion

According to this first comparison between the experimental and the simulation results, it looks like that under low sorbent flow rates the modelling accuracy is limited, especially for the absorption process. As the discrepancy between the real extracted power and the expected value is much higher for the absorption process than for the desorption process, the combination of the absorber and desorber unit can be questioned. Nevertheless, the evaporator/condenser unit works well, probably due to the fluid recirculation and in desorption modus, the A/D tube bundle under-performs the simulation by only 25 %.

In the near future, more extensive comparisons between the modelling and experiments will be carried out. In parallel, for the absorber heat and mass exchanger, the wetting should be optimised and/or a new concept should be found. One step towards this target is performing measurements on a down-scaled experimental set-up.

Acknowledgements

Financial support by the European Union in the frame of FP 7 under the grant number 295568 and of the University of Applied Sciences Rapperswil as well as of the Swiss CTI (SCCER) is gratefully acknowledged.

Received: August 10, 2016

[1] J.-C. Hadorn, 'Thermal Energy Storage for Solar and Low Energy Buildings: State of the Art', International Energy Agency, **2005**.
[2] 'Advances in Thermal Energy Storage Systems: Methods and Applications', 1st ed., Ed. L. F. Cabeza, Boston, MA: Woodhead Publishing, **2014**.
[3] R. Weber, V. Dorer, *Vacuum* **2008**, *82*, 708.
[4] J. R. Thome, 'Wolverine Engineering Data Book III', **2010**, Wolverine Tube, inc.
[5] J. F. Roques, J. F. Thome, *Heat Transf. Eng.* **2003**, *24*, 40.
[6] K. J. Kim, N. S. Berman, D. S. C. Chau, B. D. Wood, *Int. J. Refrig*. **1995**, *18*, 486.
[7] S. Deng, *Int. J. Refrig*. **1999**, *22*, 293.
[8] M. Jakob, 'Heat Transfer', Wiley, **1949**.
[9] S. Lee, 'Development of techniques for in-situ measurement of heat and mass transfer in ammonia–water absorption systems', Georgia Institute of Technology, **2007**.
[10] W. L. Owens, 'Correlation of thin film evaporation heat transfer coefficients for horizontal tubes', Miami Beach, **1978**, pp. 20–22.
[11] X. Hu, A. M. Jacobi, *J. Heat Transf.* **1996**, *118*, 616.
[12] X. Hu, A. M. Jacobi, *J. Heat Transf.* **1996**, *118*, 626.